Aromatic hydroxylation reactions by electrogenerated HO radicals: A kinetic study

Raquel Oliveira, Fátima Bento*, Dulce Geraldo

Centro de Química, Universidade do Minho, Campus de Gualtar 4710-057 Braga, Portugal

* Corresponding author Tel.: +351 253604399; fax: +351 253604382; e-mail: fbento@quimica.uminho.pt

Abstract

The oxidation of benzoic acid (BA) and of 4-hydroxybenzoic acid (4-HBA) by galvanostatic electrolysis with simultaneous oxygen evolution, using BDD or Pt as anode materials is studied. Results concerning the oxidation kinetics as well as the identification and quantification of hydroxylated products are reported. First order kinetics are used to describe the consumption rates of both compounds despite of the anode material and of the applied current density. A simple kinetic model that accounts for the anode surface coverage by HO radicals is proposed. Based on this model it is possible to correlate the apparent rate constant of the organic consumption with kinetic parameter related to the organics reactivity and to the degree of the adsorption of HO radicals to the anode surface.

Keywords:

Electrochemical oxidation; Kinetic model; Hydroxyl radical; Benzoic acid; Platinum; Boron-doped diamond

1. Introduction

Hydroxyl radical ($HO^{\bullet}$), the most reactive species among oxygen radicals, is quite relevant in different fields, such as organic synthesis [1], oxidative stress studies [2] and environmental applications [3]. Reactions of $HO^{\bullet}$ with aromatic compounds have been extensively studied. It was demonstrated that addition reactions are more likely to occur than oxidation, despite the high reducing power of HO radical, $E°(HO^{\bullet}, H^{+}/H_2O)$ = 2.72 V, pH 0 [4] and $E°(HO^{\bullet}/HO^{-})$ = 1.89 V [5], probably due to the large solvent reorganization following the electron transfer reactions.

The addition mechanism of $HO^{\bullet}$ was described as involving hydrogen atom abstraction and fast nucleophilic addition with the formation of a hydroxycyclohexadienyl radical that undergoes different reactions depending on the medium composition[6].

The production of HO radicals is an important issue that can be achieved by different approaches. Pulse radiolysis and flash photolysis are among the cleanest and most reproducible methods, yet their use is rather limited as the equipments required are not accessible to most research laboratories. In opposition, chemical methods based on disproportionation of peroxynitrous acid or on decomposition of hydrogen peroxide by metal ions, known as Fenton [7] or Fenton-like reactions [8] are the most spread method despite of fundamental questions concerning the enrollment of reagents in the oxidation process. A modification of the classic Fenton reaction, allowing for a controlled production of hydroxyl radicals, was achieved by electrochemical means. The electro-Fenton reaction allows for the generation of HO radical in a controlled manner by adjusting the homogeneous production of hydrogen peroxide and Fe(II) by means of the electrochemical reduction of oxygen and Fe(III), respectively [6,9]. Hydroxyl radicals are also formed by direct electro-oxidation of water as mediators of oxygen evolution reaction (Eqs. (1) and (2)). Although radicals formed by this process are adsorbed at the anode surface they can be involved in reactions with organic compounds as expressed by Eq. (3) [10]:

$$H_2O \longrightarrow HO^{\bullet} + H^+ + e^- \quad (1)$$

$$2\,HO^{\bullet} \longrightarrow O_2 + 2H^+ + 2e^- \quad (2)$$

$$R + n\,HO^{\bullet} \longrightarrow \text{Products} \quad (3)$$

Most of the work concerning the electrogeneration of hydroxyl radicals is aimed to the detoxification of effluents [11,12] where it is envisaged the total combustion of organic material. The reported experimental conditions include high oxidation power anodes, such as Sb-SnO_2 [13], PbO_2 [14] or BDD [15], high current densities, long electrolysis times and undivided electrochemical cells. Under these conditions an efficient decrease of the chemical oxygen demand (COD) is usually attained as CO_2 is formed in a yield approaching 100% [3,16,17,18]. The benefits associated to this method of producing of HO radicals are important due to the simplicity of the required instrumentation and also because it does not require the use of any specific reagent. Despite its great success in environmental applications, the use of this method has not been explored in other important areas such as organic synthesis or oxidative stress studies.

This paper aims to demonstrate the potentiality of this method of production of HO radicals for other application besides the elimination of organics. Experiments were performed in experimental conditions that were selected to minimize the contribution from secondary reactions and from cathodic reactions, like low concentrations of organics**,** short electrolysis times and a two-compartment electrochemical cell. Benzoic acid and 4-hydroxybenzoic acid were chosen as model compounds as they are frequently used for characterizing HO radicals mediated reactions.

2. Experimental

2.1. Chemicals

All reagents employed were of analytical grade: 3-hydroxybenzoic acid (3-HBA), 2,3-dihydroxybenzoic acid (2,3-HBA), 2,4-dihydroxybenzoic acid (2,4-HBA), 2,5-dihydroxybenzoic acid (2,5-HBA), 2,6-dihydroxybenzoic acid (2,6-HBA), 2,3,4-trihydroxybenzoic acid (2,3,4-HBA), phosphoric acid, potassium dihydrogen phosphate and dipotassium hydrogen phosphate (all from ACROS Organics), potassium ferricyanide (José Gomes Santos), potassium chloride (Fluka), benzoic acid (BA; Prolabo), 2-hydroxybenzoic acid (2-HBA;Vaz Pereira), 4-hydroxybenzoic acid (4-HBA; BDH Chemicals), 3,4-dihydroxybenzoic acid (3,4-HBA; Aldrich), 3,4,5-trihydroxybenzoic acid (3,4,5-HBA; Sigma) and methanol (Fisher Scientific).

Phosphate buffer pH 7.0 was prepared by mixing adequate amounts of dipotassium hydrogen phosphate with potassium dihydrogen phosphate, whereas phosphate buffer pH 3.5 was prepared using potassium dihydrogen phosphate and phosphoric acid. The concentration of the buffer solutions was 0.15 M.

2.2. Electrochemical measurements

Voltammetric measurements and galvanostatic electrolyses were performed using a potentiostat (Autolab type PGSTAT30, Ecochemie) controlled by GPES 4.9 software provided by Ecochemie.

2.2.1. Cyclic voltammetry

Cyclic voltammetry experiments were carried out from -0.4 to 1.0 V vs Ag/AgCl, 3 M KCl at Pt disc (area 0.63 cm^2) and from 1.0 to 2.2 V vs Ag/AgCl, 3 M KCl at a BDD disc (area 0.63 cm^2) at a scan rate of 100 mV s^{-1}. The reference electrode was an Ag/AgCl, 3 M KCl electrode (CHI111, CH Instruments, Inc.). The counter electrode was a platinum wire.

2.2.2. Electrolyses

Galvanostatic electrolyses were carried out at 50, 268, 625 and 1250 A m^{-2} in a two compartments cell separated by a glass frit membrane. The volume of the anodic compartment was 9.0 ml and the solution was mechanically stirred with a magnetic stir bar (300 rpm). Pt and BDD materials were used as anode electrodes. The Pt anode (5.6 cm^2) is made of a piece (20 mm x 10 mm) of platinum gauze (52 mesh woven from 0.1 mm diameter wire, 99.9%, from Alfa Aesar). The BDD electrode (3.0 cm^2; 15 mm x 20 mm) characterized by a 800 ppm boron concentration and a BDD-film thickness of 2.7 µm, on a substrate of monocrystalline silicon, p-doped was purchased at Adamant Technologies, Switzerland. The area of the Pt working electrode was determined using a 1.00 mM of $K_3Fe(CN)_6$ in 0.1 M KCl, in a cronoamperometry experiment. The diffusion coefficient used was 7.63 x 10^{-6} cm^2s^{-1} [19]. Before each experiment anodes were electrochemically cleaned by applying a constant current according to its nature. The Pt anode was cleaned using 0.02 A in a 0.1 M phosphate buffer pH 3.5 during 600 s, whereas the BDD anode was cleaned using -0.01 A in a 0.1 M phosphate buffer pH 7.0 for the same period of time.

Apparent constant rate was determined by the average values of at least two electrolysis and its uncertainty was estimated through the standard deviation of the slope of the straight-lines Eq. (5).

2.3. HPLC

The reactions were monitored both by the concentration decrease of BA or of 4-HBA along time and by the quantification of hydroxylated products formed at 360 s. Hydroxylated compounds were selected as relevant reactive products as they are known to be the main products formed in the presence of oxygen, as demonstrated for BA reaction with HO radicals generated by radiolysis [20,21,22], by photochemistry [23,24] and by electro-Fenton reaction [25]. These products have also been detected

as intermediaries in the photocatalytic degradation of BA induced by TiO_2 [26], in photo-Fenton oxidation of BA and in electrochemical oxidation of BA using BDD [18,27].

HPLC analyses were performed using a Jasco, PU-2080 Plus system equipped with a RP 18 column from Grace Smart (250 mm x 4.6 mm, 5 µm particle size) and Clarity HPLC software from Jasco. A flow rate of 0.6 ml min^{-1} and a loop of 20 µl were used. A mixture of methanol: water: phosphoric acid (60:39:1) (v/v) was used as mobile phase. The detection was made at 230 nm and the quantification was performed using standard curves for each substance.

3. Results and discussion

3.1. Voltammetry of benzoic acid and of 4-hydroxybenzoic acid at Pt and at BDD electrodes

The voltammetric responses of BA and of 4-HBA in phosphate buffer pH 3.5 at BDD and at Pt electrodes are presented in Fig. 1 A and B, respectively. The voltammogram of BA using BDD displays a not well-defined peak whereas the voltammogram of 4-HBA shows a well-defined peak at lower potentials. This result shows that the presence of the hydroxyl group in the aromatic ring favors the electron transfer reaction. Besides, these reactions are not reversible and the products formed tend to block the electrode surface decreasing the current in sequential runs (results not shown), as it was previously reported [18,28].

Voltammograms recorded for both compounds with the Pt electrode do not show a significant difference from those recorded in the blank solution. This result shows that the present experimental conditions did not allow the adsorption of BA or of 4-HBA for its subsequent oxidation, as it was previously demonstrated to occur under controlled conditions [29].

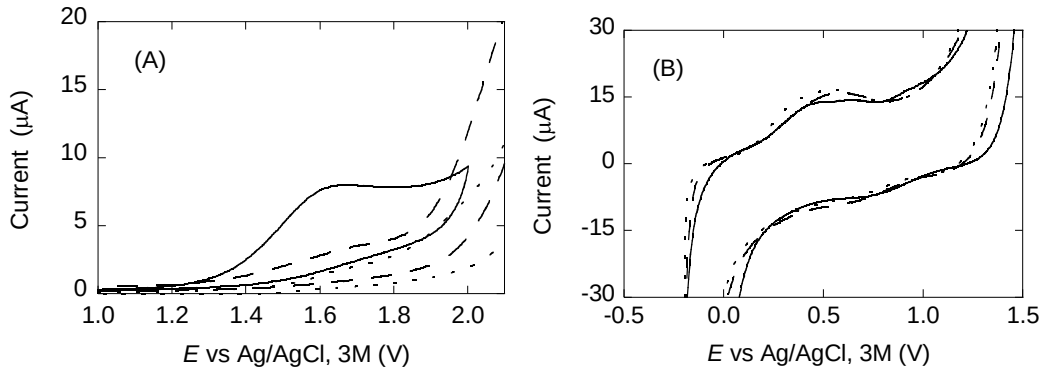

Fig. 1. Cyclic voltammograms (100 mV s^{-1}) of benzoic acid 0.50 mM (– –) and of 4-hydroxybenzoic acid 0.50 mM (—) in 0.15 M phosphate buffer solution pH 3.5, and of the blank (---) obtained at: (A) BDD and (B) Pt electrodes.

3.2. Galvanostatic electrolysis

Two sets of galvanostatic electrolyses of BA (0.50 mM) were conducted in 0.15 M phosphate buffer pH 3.5 using either a BDD anode (A = 3.0 cm^2) or a Pt anode (A = 5.6 cm^2) at a current density of 625 A m^{-2}. The concentration decrease of BA, quantified by HPLC, is expressed by means of the concentrations ratio C/C_0 and plotted against the electrolysis time, where C is the concentration of BA and C_0 its initial concentration. Results are shown in Fig. 2 A. The concentration profiles obtained using both anode materials follow a first order kinetics characterized by an exponential decay of the concentration with time according to following equations:

$$C = C_0 \exp\left(-\frac{k_{app} A}{V} t\right) \quad (4)$$

$$\frac{1}{A} \ln \frac{C}{C_0} = -\frac{k_{app}}{V} t \quad (5)$$

where, A is the anode area, V is the volume of the solution in the anodic compartment, t is time and k_{app} is the apparent rate constant that characterizes the consumption of BA. While Eq. (4) is the most common form of expressing the concentration variation with time, we chose to represent our data by Eq.(5) to normalize the concentration ratio by the anode area in order to eliminate this variable that would induce changes in the slopes due to the difference of the areas of the anodes. As V is the same for all

experiments carried out with both anodes, the value of the slopes can be compared directly as a measure of k_{app}. The slopes of the two straight-lines presented in Fig. 2 A are clearly different, (1.79 ± 0.03) x10^{-5} m s^{-1} for BDD and (3.6 ± 0.3) x10^{-6} m s^{-1} for Pt. The lower value obtained for Pt cannot be attributed to a partial blockage of this anode surface as the simultaneous oxygen evolution keeps the anode surface unobstructed. Therefore, this result indicates that k_{app} depends strongly on the anode nature. Furthermore, the fact that BA oxidation is more effective when BDD is used, can be explained by the larger reactivity of this material for $HO^{\bullet}$ mediated oxidations.

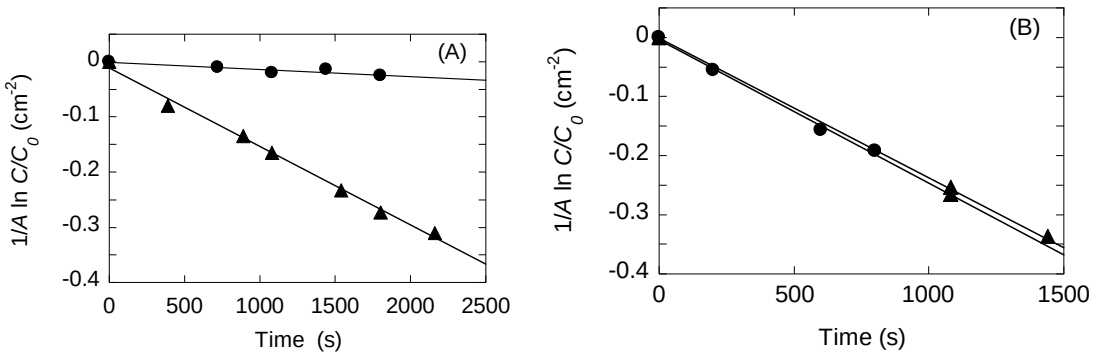

Fig. 2. Plot of the concentration decrease during galvanostatic electrolyses, linearized and normalized to the anode area: (A) BA (C_0= 0.50 mM) at Pt anode (●) ($1/A \ln(C/C_0)$ = -8.64x10^{-4} -3.60x$10^{-4}$$t$, r=0.93) and at BDD anode (▲) ($1/A \ln(C/C_0)$ = -1.08x10^{-2} - 1.79x$10^{-3}$$t$, r=0.997) and (B) 4-HBA (C_0= 0.50 mM) at Pt anode (●) ($1/A \ln(C/C_0)$ = -3.99x10^{-3} - 2.36x$10^{-3}$$t$, r=0.998) and at BDD anode (▲) ($1/A \ln(C/C_0)$ = -7.85x10^{-4} - 2.13x$10^{-3}$$t$, r= 0.9994).

The former reported experiments were repeated using 4-HBA instead of BA. The obtained results are displayed in Fig. 2 B using an identical plot. In opposition to results from BA, for 4-HBA the slopes of both straight-lines are identical (≈ (2.2±0.2) x 10^{-5} m s^{-1}, average value). In opposition to BA the k_{app} values seem not to depend on the anode material nature. Despite the use of an identical configuration of the electrochemical cell and that the solutions stirring was kept constant in all the experiments, it was not expectable that results from 4-HBA were independent on the nature of the anode material.

Comparing the slopes obtained for both compounds for the same anode material it can be concluded that k_{app} is related to nature of the organic compound. Furthermore, differences between k_{app} values are in agreement with the reactivity of the organic compounds, as k_{app} values are larger for 4-HBA (either using Pt or BDD) which is consistent with the larger reactivity of 4-HBA for electrophilic attack by $HO^{\bullet}$ [6,30]. Besides, it can be notice that there is a differentiating/leveling effect concerning the anode oxidation power when BA or 4-HBA is used. The less reactive compound discriminate the oxidation power of the two anodes, while 4-HBA, the most reactive compound, is consumed with similar rates at both anodes.

3.3. Current density effect on the rate of organics oxidation

For a better understanding of the variables that affect k_{app} galvanostatic electrolyses were carried out with BA and 4-HBA at different current densities, between 50 and 1250 A m^{-2}, at both anodes. k_{app} values were calculated for all the experiments from the analysis of the concentration decrease with time. These values are reported in Fig. 3 as a function of the applied current density. For all current densities oxygen evolution was detected at the anodes, which potential varied between 1.8 V (i = 50 A m^{-2}) and 2.6 V (i = 1250 A m^{-2}) for Pt and between 2.8 V (i = 50 A m^{-2}) and 4.6 V (i = 1250 A m^{-2}) for BDD. Values of k_{app} for both compounds follow a linear relation with the current density with an intercept that is close to zero. This effect is quite remarkable as it is observed for the two compounds and the two anode materials. Both, the linear trend and the null intercept can lead to the following conclusions.

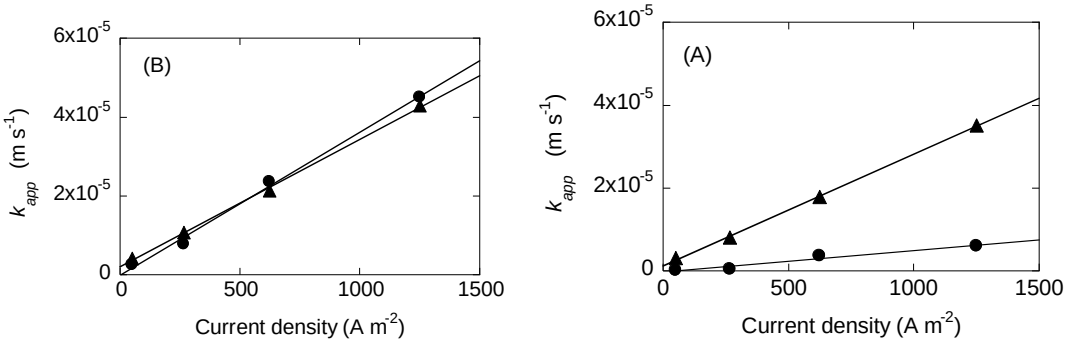

Fig. 3. Effect of current density used in the galvanostatic electrolysis on the apparent rate constant for: (A) BA (C_0 = 0.50 mM) obtained at Pt anode (●) (k_{app} = -3.13x10^{-7} + 5.26x10^{-9} i, r= 0.98) and at BDD anode (▲) (k_{app} = 1.28x10^{-6} + 2.69x10^{-8} i, r= 0.997) and (B) for 4-HBA (C_0 = 0.50 mM) obtained at Pt anode (●) (k_{app} = -1.27x10^{-7} + 3.63x10^{-8} i, r= 0.998) and at BDD anode (▲) (k_{app} = 2.09x10^{-6} + 3.23x10^{-8} i, r=0.9992).

The fact that the intercept is almost zero means that when the current approaches zero (i.e. the water decomposition process vanishes) k_{app} tends to zero, which means that the oxidation of the organic compound does not occur, even if the anode potential is always above the oxygen evolution limit. This fact provides a clear evidence on the nature of the oxidation process, as a HO$^{\bullet}$ mediated reaction and not by heterogeneous electron transfer.

The linear increase of k_{app} with the current density must be related to the increase of the surface concentration of HO radicals. The surface concentration of HO radicals must increase with the rate of the water decomposition as they are formed by this process (Eq. (1)). The importance of this effect is measured by the magnitude of the slopes. The fact that the magnitude of the slopes depend on the nature of the organic compound and of the anode material indicates that this parameter must incorporate variables associated with the reactivity of the organic species.

3.4. Analysis of hydroxylated products

Table 1 reports the results concerning the identification and quantification of the hydroxylated products formed by galvanostatic electrolysis of BA and 4-HBA with Pt

and BDD at 360 s, for the current densities of 625 A m^{-2} and of 1250 A m^{-2}. The concentration products formed at lower current densities are not reported because they were above the detection limits.

The hydroxylated products formed, assigned by the position of the hydroxyl groups, were identified by comparison of the retention times with those of the standards. The concentration of each identified hydroxybenzoic derivative is expressed as a percentage of the total concentration of hydroxybenzoic products, $[P]/\Sigma[P]$ where the total concentration of hydroxylated products is expressed as Σ [P]. The yield of hydroxylated products is quantified by the parameter $\Sigma [P]/[R]_{conv}$ where $[R]_{conv}$ is the concentration of the organic that was converted to products. Although the conversion degree of BA and 4-HBA is quite different (according to the reported values of k_{app}) and despite the difference between the anodes areas similar conclusions can be drawn concerning the effects of current density and of anode material on the yields of hydroxylated products.

The amount of hydroxylated products formed when the Pt anode was used is higher than when the BDD anode was used, as it can be observed by the values of $\Sigma [P]$ and of $\Sigma [P]/[R]_{conv}$ in Table 1. The fact that BDD seems to produce fewer hydroxylated compounds and at lower concentrations can be related to the higher activity of this anode material that might favor further oxidation of products into other forms, such as quinones, aliphatic acids and even CO_2.

On the other hand the increase of current density favors the formation of higher concentrations of hydroxylated products when Pt is used, while for BDD the concentration of products are similar for both current densities, even though higher amounts of the initial organic compound have been consumed. As a global trend the yield of hydroxylated species tend to decrease with the increase of current density indicating that hydroxylated products must be further oxidized.

3.5. Kinetic model for organics reaction with electrogenerated HO radicals

A quantitative analysis of the electrogenerated HO radicals reactions with organics must take into account the set of processes described by Eqs. (1)-(3), as previously demonstrated by Comninellis et al. [17,31]. If the organic consumption occurs solely by reaction with the HO radicals its rate of reaction can be expressed by the following rate law:

$$v_R = k_R \theta \Gamma_s C_R^E \quad (6)$$

where, v_R (mol $m^{-2}s^{-1}$) is the organic compound consumption rate, k_R ($m^3mol^{-1}s^{-1}$) the corresponding rate constant, θ the anode surface coverage by HO radicals, Γ_s (mol m^{-2}) the saturation concentration of this species and C_R^E (mol m^{-3}) is the concentration of the organic compound at the electrode surface. In order to calculate the surface concentration of HO radicals, $\theta\Gamma_s$, one has to consider the kinetics of formation (Eq. (1)) and of consumption of HO radicals, either in the formation of O_2 (Eq. (2)) or in the organics reaction (Eq. (3)). Considering that steady-state conditions are attained, an equilibrium is established between the rate of formation and the rates of consumption of these radicals:

$$v_{HO^\bullet} = 2v_{O_2} + nv_R \quad (7)$$

where $v_{HO^\bullet}$ is the rate of formation of HO radicals by water dissociation (Eq. (8)) and v_{O_2} the rate of formation of O_2 (Eq. (9)) and n is the number of HO radicals used in the reaction with the organic compound:

$$v_{HO^\bullet} = \frac{i}{zF} \quad (8)$$

$$v_{O_2} = k_{O_2} \theta \Gamma_s \quad (9)$$

From Eqs. (6) to (9) the surface concentration of HO radicals at the anode can be expressed by:

$$\theta \Gamma_s = \frac{i}{zF(2k_{O_2} + nk_R C_R^E)} \quad (10)$$

The dependence of the surface coverage with the applied current and with the rate constants of the reactions described by Eqs. (2) and (3) was previously described by an equation similar to Eq. (10) [17,31].

Following Eq. (10) the rate of the organic consumption can be expressed by:

$$v_R = \frac{k_R i}{z\mathrm{F}(2k_{O_2} + nk_R C_R^E)} C_R^E \qquad (11)$$

or by:

$$v_R = \frac{i}{z\mathrm{F}\left(\frac{2k_{O_2}}{k_R} + nC_R^E\right)} C_R^E \qquad (12)$$

Therefore the apparent rate constant can be defined as:

$$k_{app} = \frac{i}{z\mathrm{F}\left(\frac{2k_{O_2}}{k_R} + nC_R^E\right)} \qquad (13)$$

This equation predicts that the rate of the organics consumption is related with the rate constant of O_2 formation, with the rate constant of the organics reaction, with the organics concentration and also with the number of HO radicals used in the organic reaction. Two limiting situations can be define depending on the relative magnitude of C_R^E toward k_{O_2}/k_R:

For $n\ C_R^E >> 2\ k_{O_2}/k_R$,

$$(k_{app})_0 = \frac{i}{z\,\mathrm{F}\,n\,C_R^E} \qquad (14)$$

For $n\ C_R^E << 2\ k_{O_2}/k_R$,

$$(k_{app})_1 = \frac{i}{2z\,\mathrm{F}}\frac{k_R}{k_{O_2}} \qquad (15)$$

Therefore, for higher concentrations of organics Eq. (14) predicts that the apparent rate constant is a function of the applied current, of the organics concentration and of

the stoichiometric coefficient of the HO radical in Eq. (3). Under these circumstances k_{app} does not depend on the organics reactivity, k_R. This approximation can also be attained by disregarding the first term of Eq. (7), which means that the anode coverage by HO radicals depends entirely on the balance between the formation of $HO^{\bullet}$ and its use by the organics oxidation. Furthermore, the organics oxidation rate is predicted to follow a zero order reaction ($v_R = i/n\mathrm{F}$).

In opposition, for low concentrations of organics the apparent rate constant given by Eq. (15) increases with the applied current and with k_R and decreases with k_{O_2}. In this situation the surface concentration of $HO^{\bullet}$ is mainly controlled by the balance between the formation of $HO^{\bullet}$ and its consumption in O_2 evolution. Moreover, reactions are expected to follow a first order kinetics.

The concentration effect on k_{app}, computed by means of Eq. (13) is reported in Fig. 4 A for n = 18, i = 1250 A m^{-2} and for different k_{O_2}/k_R values (5, 10, 25, 150 and 500 mol m^{-3}). The deviation of k_{app} from the two limiting situations described by Eq. (14) and Eq. (15) are reported in Fig. 4 B and C, where these deviations are expressed in percentage of the limiting values $(k_{app})_0$ or $(k_{app})_1$. The selected value for n (=18) corresponds to the number of HO radicals needed to oxidize BA completely. This high number was considered as it corresponds to the less favorable situation for attaining the limiting condition expressed by Eq. (15), i.e. to verify a first order kinetics.

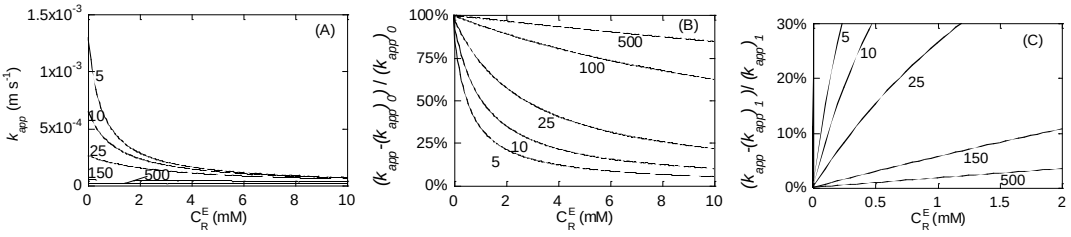

Fig. 4. Effect of concentration on: (A) the apparent rate constant, k_{app}, (B) relative deviation of k_{app} from $(k_{app})_0$ and (C) relative deviation of k_{app} from $(k_{app})_1$ evaluated for n = 18, i = 1250 A m^{-2} and k_{O_2}/k_R = 5, 10, 25, 150, 500 mol m^{-3}.

Table 1. Identification of hydroxylated products of BA and 4-HBA formed by galvanostatic electrolysis after 360 s using either Pt or BDD anodes. The initial concentration of BA and 4-HBA was 0.50 mM. Quantification of the total concentration of hydroxylated products, Σ [*P*], and of the yield of hydroxylation Σ [*P*]/[*R*]$_{conv}$. [*R*]$_{conv}$ is the concentration of R that was converted to products and [*P*] is the concentration of each identified hydroxylated product.

	i	k_{app}		$[R]_{conv}$		Σ *[P]*		Σ *[P]*/$[R]_{conv}$		x-HBA	*[P]*/ Σ*[P]*	
	A m^{-2}	(10^{-5}) m s^{-1}		mM		(10^{-2}) mM		%			%	
R		Pt	BDD	Pt	BDD	Pt	BDD	Pt	BDD		Pt	BDD
BA	625	0.360±0.003	1.79±0.03	0.0387	0.104	1.32	0.777	34	7	4-	37	45
										3,4,5-	63	55
	1250	0.61±0.02	3.51±0.03	0.0638	0.185	1.81	0.674	28	4	3-	-	8
										4-	31	44
										2,5-	22	-
										3,4-	29	-
										2,3,4-	18	-
										3,4,5-	-	48
4-HBA	625	2.4±0.4	2.13±0.08	0.287	0.268	1.11	0.0341	39	1	2,4-	1	-
										3,4-	46	43
										2,3,4-	18	-
										3,4,5-	35	57
	1250	4.5±0.4	4.3±0.9	0.401	0.393	1.32	0.0343	33	1	2,4-	8	-
										3,4-	44	90
										2,3,4-	25	10
										3,4,5-	24	-

From the reported values in Fig. 4 A one can observe that k_{app} displays a strong dependence on both concentration and k_{O_2}/k_R. The concentration effect on k_{app} tends to be more significant for lower k_{O_2}/k_R ratios. For higher k_{O_2}/k_R values k_{app} tend to be approximately constant although dependent on the ratio k_{O_2}/k_R. The relative deviation of k_{app} from $(k_{app})_0$ (Fig. 4 B) is considerable for higher values of the ratio k_{O_2}/k_R despite of the concentration. In opposition, for 5 mM solutions deviations lower than 10% can be achieved if $k_{O_2}/k_R < 5$. On the other hand the deviations of k_{app} to $(k_{app})_1$ (Fig. 4 C) tend to decrease for the higher k_{O_2}/k_R, namely deviations lower than 10% are obtained for concentrations lower than 2 mM if $k_{O_2}/k_R \geq 150$.

The deviation between k_{app} and $(k_{app})_1$ for a concentration of 1 mM as a function of current density is illustrated in Fig. 5, where the k_{app} values (solid lines) are compared to $(k_{app})_1$ (dashed lines) for different k_{O_2}/k_R , i.e. 25, 150 and 500 mol m^{-3} and n = 18 (Fig. 5 A), whereas values for k_{O_2}/k_R = 150 mol m^{-3} for different n, namely 2, 9 and 18 are reported in Fig. 5 B. Although a linear relation is always obtained, the direct assessment of k_R/k_{O_2} from the slope can be erroneous depending on both k_{O_2}/k_R and n. The magnitude of these errors can be regarded through the discrepancy between the solid and the dashed lines for identical k_{O_2}/k_R (Fig. 5 A). Deviations of about 26%, 5.7% and 1.8% are observed for k_{O_2}/k_R equal to 25, 150 and 500 mol m^{-3}, respectively. On the other hand, for k_{O_2}/k_R = 150 mol m^{-3} deviations of 5.7%, 2.9% and 0.7% are observed for n equal to 18, 9, and 2, respectively.

Besides the effect of the current density on k_{app} related to the increase of the electrode surface coverage by HO radicals, the current increase can bring additional consequences related to the mass transport efficiency. The oxygen evolution leads to the formation of small bubbles at the electrode surface which produces an additional source of convection that will certainly disrupt the diffusion layer. Therefore the current density increase can lead to an increase of the mass transport rate. Two different

situations can arise depending on the existence or not of a concentration polarization at the electrode surface. In the first situation the increase of current density will affect the concentration gradient, $C_R^S - C_R^E$ (where C_R^S is the bulk organics concentration), as convection will tend to homogenize solution. In opposition, when the concentration polarization can be neglected, i.e. $C_R^S = C_R^E$, k_{app} does not depend on the diffusion rate of the organics toward the electrode and therefore the convection increase (due to oxygen bubbles formation) associated to the current density increase should not affect k_{app}.

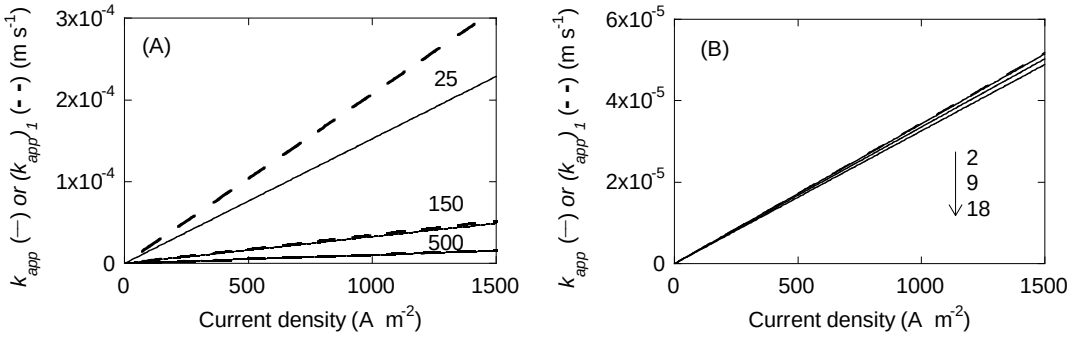

Fig. 5. Effect of current density on k_{app} (solid lines) and on $(k_{app})_1$ (dashed lines) for C_R^E =1 mM: (A) for n = 18 and k_{O_2}/k_R = 25, 150, 500 mol m^{-3} and (B) for k_{O_2}/k_R = 150 mol m^{-3} and n = 2, 9, 18.

Following the above development and considering that our experimental results followed first order kinetics, values of k_R/k_{O_2} were estimated from the experimental k_{app} of BA and of 4-HBA obtained using Pt or BDD at different current densities (Table 2). The ratio between the rate constants of the two organic compounds, $k_{4\text{-}HBA}/k_{BA}$, for the same anode were estimated from $k_{4\text{-}HBA}/k_{O_2}$ and k_{BA}/k_{O_2}values. Although this ratio is independent of the current density it depends strongly on the anode material. For Pt (a low oxidation power anode) there is a higher ratio of $k_{4\text{-}HBA}/k_{BA}$ (= 6.8) showing that there is a considerable difference between the two rate constants, whereas for BDD (a high oxidation power anode) this ratio is lower (= 1.3).

It is also noticeable that the values of $k_{4\text{-}HBA}/k_{O_2}$ and k_{BA}/k_{O_2} obtained for 50 A m^{-2} are higher than those for the higher current densities. Despite this difference the value of the ratio $k_{4\text{-}HBA}/k_{BA}$ from 50 A m^{-2} is similar to those obtained from the other current densities. The fact that the lower values of $k_{4\text{-}HBA}/k_{O_2}$ and k_{BA}/k_{O_2} were obtained for the higher current densities is not expectable considering the convection increase associated to the higher rates of oxygen evolution that occurs at the higher current densities. Therefore it can be concluded that both O_2 formation and the organics reaction were not mass transport limited. Instead, this effect can be explained considering a hindrance of the electrode surface by the O_2 bubbles that is more important for higher current densities. This effect contributes to a reduction of the available anode surface leading to a decrease of k_{app}, and consequently of $k_{4\text{-}HBA}/k_{O_2}$ and k_{BA}/k_{O_2}, nonetheless the ratios $k_{4\text{-}HBA}/k_{BA}$ are not affected.

Table 2. Values of k_{BA}/k_{O_2} and *of* $k_{4\text{-}HBA}/k_{O_2}$ estimated from k_{app} of BA and 4-HBA for the two anodes at different current densities. $k_{4\text{-}HBA}/k_{BA}$ corresponds to the ratio $(k_{4\text{-}HBA}/k_{O_2})/(k_{BA}/k_{O_2})$.

	Pt			BDD		
i (Am^{-2})	k_{BA}/k_{O_2} (m^3mol^{-1})	$k_{4\text{-}HBA}/k_{O_2}$ (m^3mol^{-1})	$k_{4\text{-}HBA}/k_{BA}$	k_{BA}/k_{O_2} (m^3mol^{-1})	$k_{4\text{-}HBA}/k_{O_2}$ (m^3mol^{-1})	$k_{4\text{-}HBA}/k_{BA}$
50	$(1.45\pm0.08)\times10^{-3}$	$(9.9\pm0.02)\times10^{-3}$	6.9	$(1.18\pm0.05)\times10^{-2}$	$(1.6\pm0.1)\times10^{-2}$	1.4
268	$(8.7\pm0.5)\times10^{-4}$	$(6\pm1)\times10^{-3}$	6.5	$(5.8\pm0.2)\times10^{-3}$	$(8\pm2)\times10^{-3}$	1.3
625	$(1.11\pm0.01)\times10^{-3}$	$(7\pm1)\times10^{-3}$	6.6	$(5.53\pm0.09)\times10^{-3}$	$(6.6\pm0.2)\times10^{-3}$	1.2
1250	$(9.4\pm0.2)\times10^{-4}$	$(6.9\pm0.6)\times10^{-3}$	7.4	$(5.42\pm0.05)\times10^{-3}$	$(7\pm1)\times10^{-3}$	1.2

4. Conclusions

The oxidation of BA and of 4-HBA by galvanostatic electrolysis with simultaneous oxygen evolution, using BDD or Pt as anode materials are examined. The products formed from the oxidation of the two organic compounds at the two anodes include hydroxylated derivatives that are typical of HO radicals reactions. The yields of hydroxylated products were rather low for BDD as compared with those obtained when

the Pt anode was used. The concentration decrease of BA and of 4-HBA follows first[t] order kinetics characterized by an apparent rate constant, k_{app}, that depends on the anode material and on the current density used in the electrolysis. The existence of a direct proportionality between k_{app} and the current density demonstrates that the reaction does not occur when the production of O_2 does not take place, despite the high potential of the anode in all experiments. Therefore it was concluded that the oxidations of either BA or 4-HBA are started by HO radicals whose formation only takes place in conditions where O_2 is produced. A simple kinetic model that accounts for the anode surface coverage by HO radicals is proposed to interpret these results. This model predicts two limiting situations according to the magnitude of the organics concentration in comparison with the ratio of the rate constants k_{O_2}/k_R. For higher concentrations it is predicted that the rate of the organics consumption is independent of both its concentration and its reactivity, whereas for lower concentrations first order kinetics is envisaged. Based on this model the ratios k_{BA}/k_{O_2}, $k_{4\text{-}HBA}/k_{O_2}$ and $k_{4\text{-}HBA}/k_{BA}$ are estimated from experiments carried out with the two anode materials. The calculated reactivity ratio $k_{4\text{-}HBA}/k_{BA}$ is higher than 1 as expected due to the higher reactivity of the hydroxylated derivative. Furthermore, a higher ratio is obtained for experiments carried out with platinum, which is also likely to occur due to the higher adsorption strength of HO radicals at this material, allowing for a better differentiation of the reactivity of organics.

Acknowledgments

Thanks are due to FCT (Fundação para a Ciência e Tecnologia) and FEDER (European Fund for Regional Development)-COMPETE-QREN-EU for financial support to the Research Centre, CQ/UM [PEst-C/QUI/UI0686/2011 (FCOMP-01-0124-FEDER-022716)]. Raquel Oliveira thanks to FCT, POPH (Programa Operacional Potencial Humano) and FSE (Fundo Social Europeu) for the PhD Grant (SFRH/BD/64189/2009).

References

[1] T.F.S. Silva, K.V. Luzyanin, M.V. Kirillova, M.F.G. da Silva, L.M.D.R.S. Martins, A.J.L. Pombeiro, Novel Scorpionate and Pyrazole Dioxovanadium Complexes, Catalysts for Carboxylation and Peroxidative Oxidation of Alkanes, Advanced Synthesis & Catalysis 352 (2010) 171-187.

[2] J.V. Hunt, R.T. Dean, S.P. Wolff, Hydroxyl Radical Production and Autoxidative Glycosylation - Glucose Autoxidation as the Cause of Protein Damage in the Experimental Glycation Model of Diabetes-Mellitus and Aging, Biochemical Journal 256 (1988) 205-212.

[3] C. Comninellis, Electrocatalysis in the Electrochemical Conversion/Combustion of Organic Pollutants for Waste-Water Treatment, Electrochimica Acta 39 (1994) 1857-1862.

[4] H.A. Schwarz, R.W. Dodson, Equilibrium between hydroxyl radicals and thallium(II) and the oxidation potential of hydroxyl(aq), The Journal of Physical Chemistry 88 (1984) 3643-3647.

[5] D.T. Sawyer, J.L. Roberts, Hydroxide Ion - an Effective One-Electron Reducing Agent, Accounts of Chemical Research 21 (1988) 469-476.

[6] M.A. Oturan, J. Pinson, Hydroxylation by Electrochemically Generated Oh Radicals - Monohydroxylation and Polyhydroxylation of Benzoic-Acid - Products and Isomers Distribution, Journal of Physical Chemistry 99 (1995) 13948-13954.

[7] L.M. Dorfman, Reactivity of the hydroxyl radical in aqueous solutions [electronic resource] / Leon M. Dorfman and Gerald E. Adams, U.S. Dept. of Commerce, National Bureau of Standards, [Washington, D.C.] :, 1973.

[8] J.A. Simpson, K.H. Cheeseman, S.E. Smith, R.T. Dean, Free-Radical Generation by Copper Ions and Hydrogen-Peroxide - Stimulation by Hepes Buffer, Biochemical Journal 254 (1988) 519-523.

[9] A. Ventura, G. Jacquet, A. Bermond, V. Camel, Electrochemical generation of the Fenton's reagent: application to atrazine degradation, Water Research 36 (2002) 3517-3522.

[10] A. Kapalka, G. Foti, C. Comninellis, The importance of electrode material in environmental electrochemistry Formation and reactivity of free hydroxyl radicals on boron-doped diamond electrodes, Electrochimica Acta 54 (2009) 2018-2023.

[11] C.A. Martinez-Huitle, E. Brillas, Decontamination of wastewaters containing synthetic organic dyes by electrochemical methods: A general review, Applied Catalysis B-Environmental 87 (2009) 105-145.

[12] C.A. Martinez-Huitle, F. Hernandez, S. Ferro, M.A.Q. Alfaro, A. de Battisti, Electrochemical oxidation: An alternative for the wastewater treatment with organic pollutants agents, Afinidad 62 (2006) 26-34.

[13] C. Borras, C. Berzoy, J. Mostany, J.C. Herrera, B.R. Scharifker, A comparison of the electrooxidation kinetics of p-methoxyphenol and p-nitrophenol on Sb-doped SnO2 surfaces: Concentration and temperature effects, Applied Catalysis B: Environmental 72 (2007) 98-104.

[14] P.G. Keech, N.J. Bunce, Electrochemical oxidation of simple indoles at a PbO2 anode, Journal of Applied Electrochemistry 33 (2003) 79-83.

[15] J. Iniesta, P.A. Michaud, M. Panizza, G. Cerisola, A. Aldaz, C. Comninellis, Electrochemical oxidation of phenol at boron-doped diamond electrode, Electrochimica Acta 46 (2001) 3573-3578.

[16] A. Kapalka, G. Foti, C. Comninellis, Kinetic modelling of the electrochemical mineralization of organic pollutants for wastewater treatment, Journal of Applied Electrochemistry 38 (2008) 7-16.

[17] O. Simond, V. Schaller, C. Comninellis, Theoretical model for the anodic oxidation of organics on metal oxide electrodes, Electrochimica Acta 42 (1997) 2009-2012.
[18] F. Montilla, P.A. Michaud, E. Morallon, J.L. Vazquez, C. Comninellis, Electrochemical oxidation of benzoic acid at boron-doped diamond electrodes, Electrochimica Acta 47 (2002) 3509-3513.
[19] J.E. Baur, in: C.G. Zoski (Ed.), Handbook of Electrochemistry, Elsevier B.V, Amsterdam, 2007, pp. 829-848.
[20] I. Loeff, A.J. Swallow, On Radiation Chemistry of Concentrated Aqueous Solutions of Sodium Benzoate, Journal of Physical Chemistry 68 (1964) 2470-&.
[21] G.W. Klein, K. Bhatia, V. Madhavan, R.H. Schuler, Reaction of Oh with Benzoic-Acid - Isomer Distribution in Radical Intermediates, Journal of Physical Chemistry 79 (1975) 1767-1774.
[22] A.M. Downes, The Radiation Chemistry of Aqueous Solutions of [C-14]Benzoic and [C-14]Salicylic Acids, Australian Journal of Chemistry 11 (1958) 154-157.
[23] H.G.C. Bates, N. Uri, Oxidation of Aromatic Compounds in Aqueous Solution by Free Radicals Produced by Photo-Excited Electron Transfer in Iron Complexes, Journal of the American Chemical Society 75 (1953) 2754-2759.
[24] C.R.E. Jefcoate, J.R.L. Smith, R.O.C. Norman, Hydroxylation. Part IV. Oxidation of some benzenoid compounds by Fenton's reagent and the ultraviolet irradiation of hydrogen peroxide, Journal of the Chemical Society B: Physical Organic (1969) 1013-1018.
[25] M.A. Oturan, J. Pinson, Hydroxylation by Electrochemically Generated OH.bul. Radicals. Mono- and Polyhydroxylation of Benzoic Acid: Products and Isomer Distribution, The Journal of Physical Chemistry 99 (1995) 13948-13954.
[26] T. Velegraki, D. Mantzavinos, Conversion of benzoic acid during TiO2-mediated photocatalytic degradation in water, Chemical Engineering Journal 140 (2008) 15-21.
[27] T. Velegraki, G. Balayiannis, E. Diamadopoulos, A. Katsaounis, D. Mantzavinos, Electrochemical oxidation of benzoic acid in water over boron-doped diamond electrodes: Statistical analysis of key operating parameters, kinetic modeling, reaction by-products and ecotoxicity, Chemical Engineering Journal 160 (2010) 538-548.
[28] B. Louhichi, N. Bensalash, A. Gadri, Electrochemical oxidation of benzoic acid derivatives on boron doped diamond: Voltammetric study and galvanostatic electrolyses, Chemical Engineering & Technology 29 (2006) 944-950.
[29] R.M. Souto, J.L. Rodriguez, L. Fernandez-Merida, E. Pastor, Electrochemical reactions of benzoic acid on platinum and palladium studied by DEMS. Comparison with benzyl alcohol, Journal of Electroanalytical Chemistry 494 (2000) 127-135.
[30] M.I. Pariente, F. Martinez, J.A. Melero, J.A. Botas, T. Velegraki, N.P. Xekoukoulotakis, D. Mantzavinos, Heterogeneous photo-Fenton oxidation of benzoic acid in water: Effect of operating conditions, reaction by-products and coupling with biological treatment, Applied Catalysis B-Environmental 85 (2008) 24-32.
[31] G. Foti, C. Comninellis, Electrochemical oxidation of organics on iridium oxide and synthetic diamond based electrodes, in: R. White (Ed.), Modern Aspects of Electrochemistry, New York: Plenum Press, 2004, pp. 87-130.